Marsh sedimentation controls delta top morphology, slope, and mass balance

Kelly Marie Sanks[1], Samuel M Zapp[2], Jose Silvestre[3], John Shaw[4], Ripul Dutt[1], and Kyle Martin Straub[1]

[1]Tulane University
[2]Louisiana State University
[3]Tulane
[4]University of Arkansas at Fayetteville

November 22, 2022

Abstract

Rising sea levels, subsidence, and decreased fluvial sediment load threaten river deltas and their marshes. However, the feedbacks between fluvial and marsh deposition remain weakly constrained. We investigate how marsh accumulation impacts the fluvial sediment partitioning between a delta's topset, coastal zone, and foreset by comparing a delta experiment with proxy marsh accumulation to a control. Marsh accumulation alters fluvial sediment distribution by decreasing the slope in the subaerial marsh window by ~40%, creating an ~8% larger delta top and a ~100% larger marsh platform. The reduced slopes decrease relative delta elevation, and fluvial incursions into the marsh trap 1.3 times more clastic volume. The volume exported to deep water remains unchanged. Marsh deposition shifts elevation distributions towards sea level, which produces a hypsometry akin to field-scale deltas. Given that risk is tied to elevation, marsh accumulation accentuates low-elevation areas, while providing essential land-building capabilities.

Marsh sedimentation controls delta top morphology, slope, and mass balance

K. M. Sanks[1,3], S. M. Zapp[1,2], J. R. Silvestre[3], J. B. Shaw[1], R. Dutt[3], and K. M. Straub[3*]

[1]University of Arkansas, Department of Geoscience, 340 N. Campus Drive, 216 Gearhart Hall, Fayetteville, AR 72701
[2]United States Geological Survey, Lower Mississippi Gulf Water Science Center, 700 W. Research Center Blvd, Fayetteville, AR 72701
[2]Louisiana State University, Department of Oceanography and Coastal Sciences, 1002-Y Energy, Coast and Environment Building, Baton Rouge, LA 70803
[3]Tulane University, Department of Earth and Environmental Sciences, 6823 St. Charles Avenue, Blessey Hall, New Orleans, LA 70118

Key Points:

- Marsh deposition decreases delta slope, creating feedbacks that alter the spatial deposition of clastic material
- The interaction of marsh and clastic deposition creates a delta hypsometry more akin to global deltas than experiments without marsh
- Delta-marsh interactions generate large extents of land near sea level, making this interaction key to managing deltaic landscapes

*Funded by National Science Foundation and the U.S. Geological Survey.

Corresponding author: Kelly Sanks, ksanks@tulane.edu

Abstract

Rising sea levels, subsidence, and decreased fluvial sediment load threaten river deltas and their marshes. However, the feedbacks between fluvial and marsh deposition remain weakly constrained. We investigate how marsh accumulation impacts the fluvial sediment partitioning between a delta's topset, coastal zone, and foreset by comparing a delta experiment with proxy marsh accumulation to a control. Marsh accumulation alters fluvial sediment distribution by decreasing the slope in the subaerial marsh window by ∼40%, creating an ∼8% larger delta top and a ∼100% larger marsh platform. The reduced slopes decrease relative delta elevation, and fluvial incursions into the marsh trap 1.3 times more clastic volume. The volume exported to deep water remains unchanged. Marsh deposition shifts elevation distributions towards sea level, which produces a hypsometry akin to field-scale deltas. Given that risk is tied to elevation, marsh accumulation accentuates low-elevation areas, while providing essential land-building capabilities.

Plain Language Summary

Low-lying deltaic coastal zones, often with abundant vegetation (wetlands), are threatened worldwide because of rising sea level and decreased sediment supply of large rivers flowing to coastal regions. The accumulation of sediment in low-lying coastal areas is a fundamental process that helps these regions keep pace with rising sea level. This sediment may be delivered from rivers that deposit their sediment when they reach the coast, from off-shore through tides and waves, and/or through the production of plant material. Our study shows that sediment accumulated in coastal wetlands alters the elevation distribution of coastal regions and the spatial deposition of the river sediment. These results provide important information for future plans to help regain coastal land area.

1 Introduction

River deltas and their marsh platforms are diverse ecosystems threatened by anthropogenic impacts to coastal areas, such as rising sea levels, subsidence, and leveeing of channels (Ericson et al., 2006). Organic material production, a critical form of sediment accumulation in many river deltas, is the primary driver of marsh platform growth (Nyman et al., 2006), whereas clastic sedimentation via rivers drives deltaic lobe growth (Edmonds et al., 2009). To successfully predict the long-term fate of these ecosystems, the interaction controlling delta and marsh growth must be understood (Paola et al., 2011). While much is known about surface processes in channelized portions of river deltas (Edmonds & Slingerland, 2008; Q. Li et al., 2017; Smart & Moruzzi, 1971) and much is known about sediment accumulation in marshes (Allen, 2000; Kirwan & Murray, 2007; Morris et al., 2002), the manner in which they interact remains largely uninvestigated.

Aerial imagery and the stratigraphic record show evidence of delta-marsh interaction in modern and ancient systems, and it is well known that deltaic channel deposits are sensitive to the deposition of fine-grained and organic material in floodplains (Bohacs & Suter, 1997; Esposito et al., 2017; Hoyal & Sheets, 2009). For example, ∼25% of the recent Mississippi River Delta sedimentation was organic marsh material (by mass) (Holmquist et al., 2018; Sanks et al., 2020). Further, evidence preserved in strata suggests organic-rich deposition influenced deltaic processes over most of the Phanerozoic (Chesnut & Greb, 1992). Both modern and ancient records suggest that clastic inputs influence the stability and growth of the marsh platform, thus influencing coastal sustainability.

Previous experimental and numerical studies have added cohesion to show that vegetation influences river deltas (Hoyal & Sheets, 2009; Q. Li et al., 2017). While increased cohesion was necessary to understand the evolution of deltaic systems, a key component of deltaic sediment accumulation is neglected from these previous studies: marsh sediment accumulation. This sediment accumulates in low-lying regions of deltas worldwide and supplements clastic deposition. Marsh sediment includes both mineral and organic sediment (Sanks et al., 2020). The organic component is formed in-situ via primary production of plants and accumulates as a parabolic function of elevation relative to sea level, with maximum production occurring around mean high tide (Morris et al., 2002).

Here, we investigate the influence of marsh accumulation on delta morphology and mass balance by comparing two physical experiments conducted at the Tulane University Sediment Dynamics Laboratory. We incorporate proxy-marsh sediment accumulation in an experimental river delta, an important advance in experimental sedimentology and delta restoration. We compare this experiment to a previous, identical experiment that formed without marsh sedimentation. This setup is ideal to understand the interaction of ecogeomorphic processes in coastal marshes and physical processes of river deltas due to the ability to assess long-term behavior at reduced time and length scales, control on forcing conditions (supporting information, Table 1), precise measurements, and autogenic dynamics (Paola et al., 2009). By analyzing the experiments over long timescales relative to autogenic dynamics, we can interpret any differences as direct results of marsh deposition.

2 Materials and Methods

2.1 Experimental Setup and Data

We investigate two experimental deltas formed under identical boundary conditions. The only difference is that the control experiment evolved without explicit marsh sedimentation, while the treatment experiment evolved with the presence of marsh sedimentation (supporting information, Table 1). Both experiments were run for 560 hours ($\sim$10 times the compensation timescale), which captures many channel avulsions and inherent stochasticity of the system (Straub et al., 2009). LiDAR scans of the basin were collected every one (control) or two (treatment) hours while the experiments were paused. Aerial imagery was taken every 15 minutes.

The deposit was sectioned from distal to proximal along strike every 10 cm. We use image processing to obtain a stratigraphic marsh fraction roughly every 10 cm in strike (supporting information, Figure 1), which was interpolated across the basin using Bayesian kriging techniques to estimate the marsh and clastic volume sequestered in the basin (supporting information).

2.2 Marsh Proxy

We use a physical delta experiment coupled with simulated organic material production (marsh proxy) to understand the interactions of river deltas and their marsh platforms (Figure 1a). For simplicity, the marsh proxy simulated only the sediment properties of organic material, neglecting some physical properties of vegetation (e.g., stem density). We use kaolinite (clay) as the marsh proxy, which has a low initial bulk density ($\sim$90% porosity when deposited in water), uniform deposition upon settling, and relatively high settling velocity when surfactant (Jet Dry) is mixed into the water. Further, a distinctly different grain size and color from the riverine sediment makes it ideal to analyze in aerial imagery (Figure 1a) and stratigraphy. Note that while we discuss this proxy in terms of organic sedimentation, it may also represent fine-grained deposition deposited via non-riverine processes (e.g., tides, waves, and storms) in tidal flats and wetland platforms. Thus, representing any elevation-based, non-riverine coastal accumulation.

To first order, marshes accumulate as a function of elevation relative to sea level (rsl) (Morris et al., 2002; Cahoon et al., 1995; Baustian et al., 2012; Kirwan et al., 2010). This generalization simplifies many complex processes of marsh ecology (Morris et al., 2002) and trapping of fine sediment (S. Li et al., 2009), yet the vast swaths of coastal marsh within decimeters of sea level show that this is a dominant, emergent control. We simplify the marsh production model from Morris et al. (2002), which shows an optimum accumulation rate near mean water levels and suboptimal accumulation above and below. The experimental system was scaled to the emergent channel depth (∼14 mm). Hence, generating three elevation zones that received marsh: -9 to -5 mm rsl (unstable), -5 to 0 mm rsl (maximum production), and 0 to 5 mm rsl (stable), and collectively represent the marsh window. The maximum production zone received enough kaolinite to accumulate ∼1 times the base relative sea level rise rate ($RSLR_b$; 0.5 mm/2-hrs). The unstable and stable zones received enough sediment to accumulate $\sim 0.5 RSLR_b$ (Figure 1b).

LiDAR scans taken while the experiment was paused provide median elevation of 146.14 cm^2 hexagonal grid cells (7.5 cm sides), which determine the marsh window (Figure 1c). If the median elevation of a hexagonal bin falls in the marsh zone, we deposit either 3.4 g (maximum production zone) or 1.7 g (stable and unstable zones) of kaolinite. The marsh sediment dispenser (a sieve) is attached to a cart that moves about the basin. Deposition is promoted by using a ButtKicker™ to vibrate the sieve (black box left of sieve in Figure 1a), triggering kaolinite to rain down on the delta top. On average, we deposit the marsh proxy with ∼50% accuracy (Figure 1d; ∼60 g/hr less than the modeled rate). While less accurate than anticipated, in-situ deposition of kaolinite still provides a reasonable proxy for marsh accumulation, as shown by significantly altered morphology and clastic deposition in the treatment experiment compared to the control.

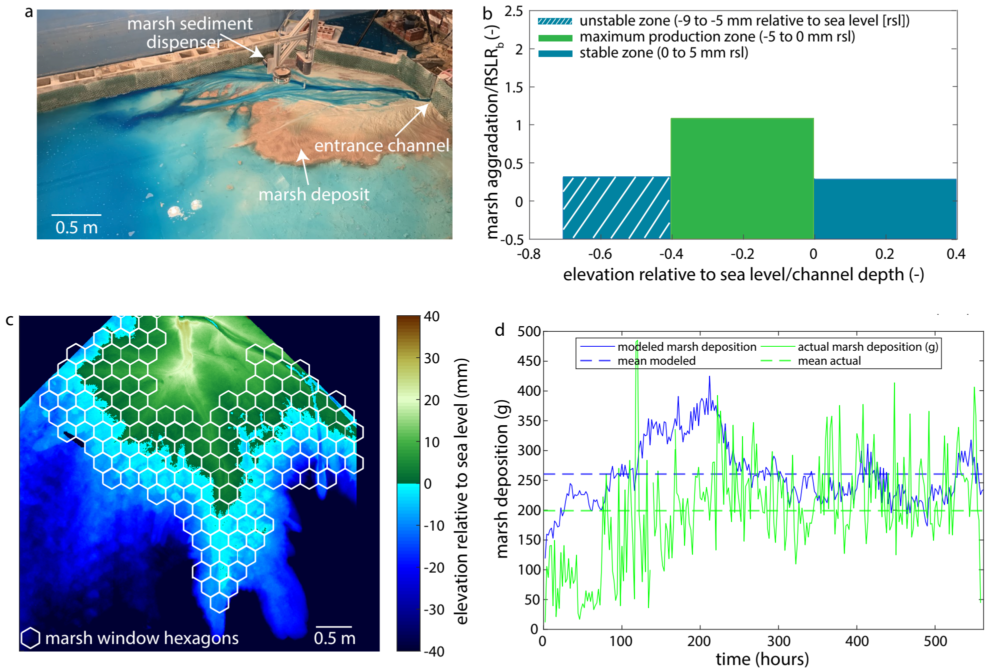

Figure 1: (a) The silver cart (top of image) holds the marsh sediment dispenser, which deposits kaolinite at the center of each hexagonal grid (c) with an average elevation in the marsh window every two hours. The brown sediment is the kaolinite marsh proxy. (b) The model, adapted from Morris et al. (2002), used to determine the marsh zone. (c) The hexagonal grid imposed upon a LiDAR scan of the basin (hour 250). (d) The modeled vs. actual marsh deposition (g) each hour during the experiment.

3 Results

3.1 Delta Morphology

A significant difference between treatment and control is observed in the area within the marsh window (5 to -9 mm rsl) and the total delta top ($\geq$-9 mm rsl). The marsh window was 0.936 ± 0.202 m^2 in the control, but larger in the treatment at an average size of 1.67 ± 0.288 m^2 (Figure 2a). Similarly, the delta top was smaller in the control at an average size of 2.80 ± 0.383 compared to 3.08 ± 0.316 m^2 for the treatment (Figure 2a). Considering the average delta top area, the treatment experiment was 10% larger than the control experiment, while the treatment marsh window was 78% larger.

The elevation distribution shows an increase in elevations within the marsh window in the treatment experiment (Figure 2b), suggesting a change in slope relative to the control. We measure slopes above the marsh window and in the subaerial marsh window radially from the apex, and observe no change in slope above the marsh ($\sim$3.0% in both experiments). Interestingly, the slope in the sub-aerial marsh window (0 to 5 mm rsl to ensure no subaqueous distortion) is significantly reduced from 3.2% in the control to 2.4% in the treatment experiment (Figure 2c).

The mean elevation as a function of radial distance from the entrance channel shows that the addition of the marsh proxy alters the elevation distribution of the delta top (Figure 2d). The treatment experiment has an increase in marsh window elevations and a decrease in the area of elevations above the marsh window. The relative elevations above the marsh window are also smaller (by about one channel depth on average). Further, the delta top slope decreases upon entrance to the marsh window in the treatment, which allows the marsh to persist over a greater distance.

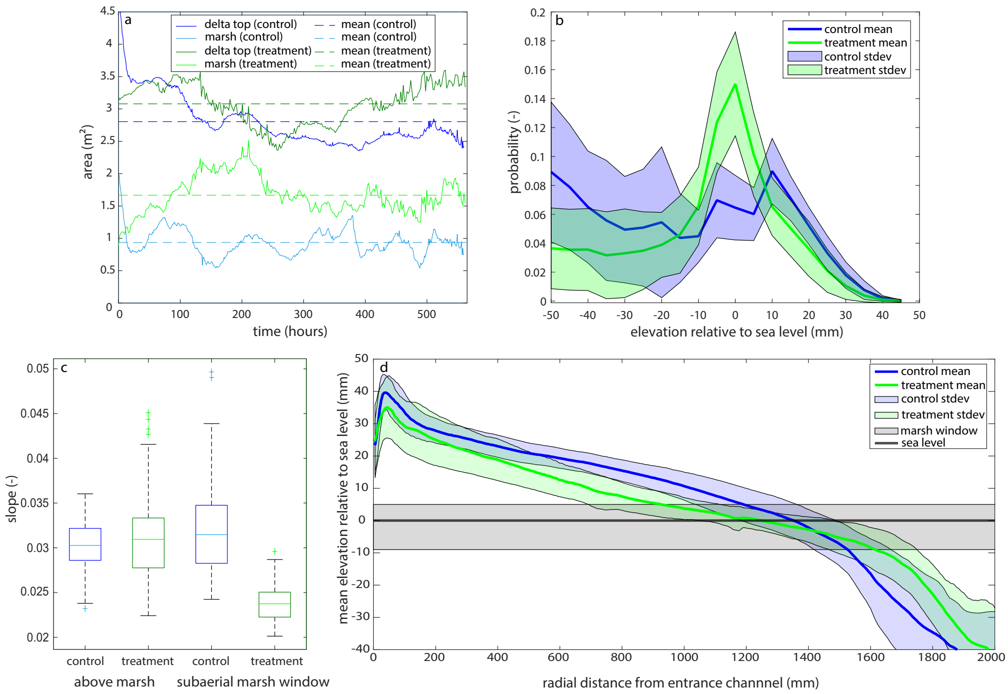

Figure 2: (a) Delta top ($\geq$ -9 mm rsl) and marsh window (-9 to 5 mm rsl) area for the control and treatment through time. (b) Time-integrated mean probability distribution of elevations relative to sea level, with one standard deviation shown for both experiments. (c) Box plots showing the time distribution of above marsh and subaerial marsh window delta slopes. (d) Mean elevation (mm) as a function of radial distance from the entrance channel (mm) integrated over space and time, with one standard deviation shown for both experiments.

3.2 Sediment Balance

While each experiment had the same clastic sediment input, the spatial distribution of sediment accumulation is different (Figure 3). For volume balance and trapping efficiency equations refer to supporting information section 2.2. We compare the area that is above the marsh window for at least 90% of the experiment to the area that is in the marsh window for less than 10% of the experiment. We choose these two zones for comparison to limit delta-marsh interaction above the marsh window and compare two distinct areas with no overlap. The area above the marsh window for greater than 90% of the control experiment is 0.880 m^2, which accumulates 0.121 m^3 of sediment throughout the experiment (Figure 3a; yellow area). The corresponding area of the treatment experiment is 0.352 m^2, which accumulates 0.0413 m^3 of clastic sediment during the experiment (Figure 3b; yellow area). Since the marsh extent is larger in the treatment experiment (Figure 3a and b; turquoise area), more clastic sediment is trapped in this elevation window than in the control. Thus, the marsh window has a 68.6% trapping efficiency (clastic sediment delivered to the delta top/clastic sediment accumulated in marsh) in the treatment, but a 51.4% trapping efficiency in the control (Table 1).

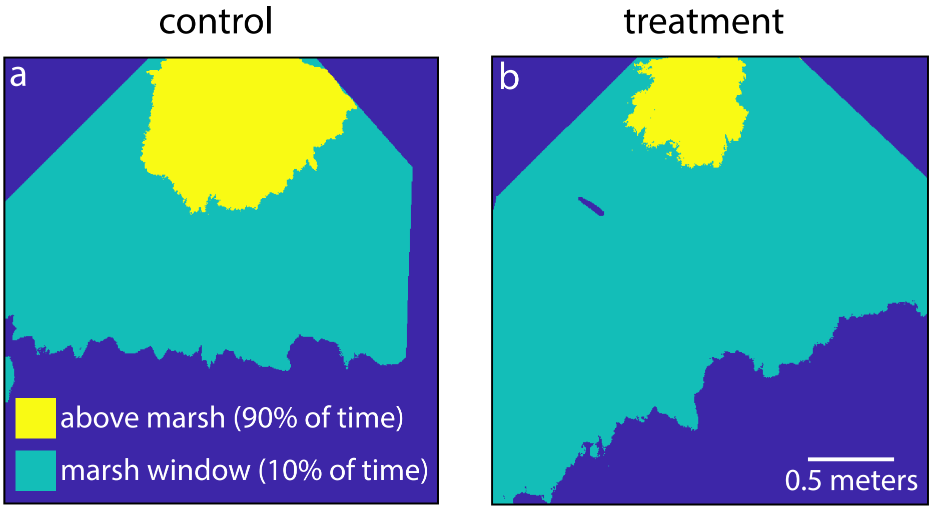

Figure 3: (a and b) The yellow area represents the area above 5 mm (above the marsh) for at least 90% of the (a) control and (b) treatment experiments, while the turquoise area represents the area in the marsh window (-9 to 5 mm) for greater than 10% of the experiment.

The area on the delta top (≥-9 mm rsl) for at least 50% of the control experiment is 2.73 m^2, accumulating a total volume of 0.363 m^3 of sediment. The corresponding area of the treatment experiment is slightly larger (2.96 m^2), but accumulates a less clastic sediment (0.355 m^3). The delta top area is smaller than the combined area shown in Figure 3, as the relative time on the delta top (≥50% of experiment) and marsh window (>10% of experiment) are different. We make this distinction here to compare average delta top conditions between the two experiments. Compared to the total fluvial input (0.660 m^3), this yields similar delta top trapping efficiencies of 55.0% in the control and 53.7% in the treatment (Table 1). Hence, similar amounts of clastic sediment are transported past the marsh zone. We also find that roughly 85% of the marsh deposited was preserved in the resulting delta top stratigraphy, which accounts for 15% of the delta top volume. Though the total clastic sediment sequestrated here is similar in both experiments, marsh sedimentation augments the clastic sedimentation in the treatment experiment leading to the formation of a vastly different delta.

Table 1: The clastic volume balance and trapping efficiency of different delta regions for the control and treatment experiments. Note that treatment marsh sedimentation is excluded.

Delta Region	**Clastic volume (m^3) [control]**	**Clastic volume (m^3) [treatment]**	**Trapping efficiency (%) [control]**	**Trapping efficiency (%) [treatment]**
delta top ($\geq$-9 mm rsl; 50% of time)	0.363	0.355	55.0	53.7
above marsh (>5 mm rsl; 90% of time)	0.121	0.0413	18.3	6.25
marsh window (-9 to 5 mm rsl; 10% of time)	0.339	0.453	51.4 [63.9[a]]	68.6 [73.2[a]]
off shore (<-9 mm rsl; 50% of time)	0.297	0.306	100	100

[a]The trapping efficiency calculated using the volume of clastic sediment delivered to the marsh window instead of the clastic sediment delivered to the delta top. Refer to supporting information section 2.2 for equations and explanation related to this difference.

4 Discussion

The experiments show that marshes interact with deltas and have first-order impacts on morphology and sediment partitioning. We show that even a small addition of marsh proxy sediment (∼8% of riverine mass) drastically impacts delta formation. Specifically, marsh deposition flattens the delta, alters location of maximum clastic deposition, and changes the delta hypsometry.

4.1 An important feedback

It is remarkable that an 8% addition of marsh mass creates a ∼100% increase in extent of the marsh window. This marsh sedimentation is essential to the long-term stability of the treatment experiment. Paradoxically, the addition of marsh proxy reduces total clastic sedimentation on the delta top, but simultaneously bridges the gap to create a delta spanning a similar extent. This illustrates an important and previously unexplored feedback between marsh and river delta sediment accumulation.

The emergent effect of the interaction between marsh and clastic sedimentation is the decreased slope of the subaerial marsh window. The flattening within the marsh window and accumulation of marsh proxy sediment here simultaneously created a 10% larger delta top (Figure 2a), but with a ∼100% larger marsh window. Because the treatment experiment has smaller slopes from the shoreline to the top of the marsh window and the shoreline location changes only slightly (Figure 2d), the area from the top of the marsh window to the apex must be smaller in the treatment experiment (Figure 2d). Marshes do not erode sediment from upstream to include within the marsh window, yet the lower slopes of a marsh in dynamic equilibrium with its delta effectively "steal" clastic sediment from higher elevations. For example, the area above the marsh accumulated 3 times less clastic volume in the treatment experiment (Table 1). Instead, the remaining sediment trapped on the delta top is sequestered in the marsh window, which accumulates 1.3 times more clastic volume (Table 1) than the control. While marsh deposition changes the sediment balance between the marsh window and elevations above it, the clastic sediment partitioning of the topset and foreset remains similar. Even so, the decreased slope and associated feedbacks leads to variation in spatial clastic deposition in the treatment experiment as compared to the control.

Decreased delta top slopes have previously been shown to alter delta morphology and increase channelization (Parker et al., 1998). Decreased delta slopes are a function of grain size and cohesion (Caldwell & Edmonds, 2014; Q. Li et al., 2017; Edmonds & Slingerland, 2010), as well as a function of the ratio of water to sediment discharge (Whipple et al., 1998; Powell et al., 2012; Wickert et al., 2013). Here we suggest a new mechanism for lowering delta top slope: non-riverine sedimentation in the floodplain. The slope break caused by marshes has been shown to influence avulsion locations (Ratliff et al., 2021). Hence, this process matters for modern-day and ancient river deltas, which often support large swaths of marsh.

4.2 Delta hypsometry

Equilibrium hypsometry, or the elevation distribution on the delta top, shows enhanced areas of elevations near sea level where marsh sedimentation or similar processes are present (Figure 2b). Using the ETOPO Global Relief Model (NOAA) in Google Earth Engine, we explore this hypothesis for four large river deltas (Mississippi River Delta, Ganges Brahmaputra Meghna Delta, Mekong River Delta, and Rio Grande River Delta). Despite coarse resolution and systematic errors in this DEM (Minderhoud et al., 2019), comparison at the vertical scale of several meters is appropriate (supporting information section 3, Figure 2). Scaling by channel depth (for comparison across scales) reveals the general hypsometry of these deltas (Figure 4).

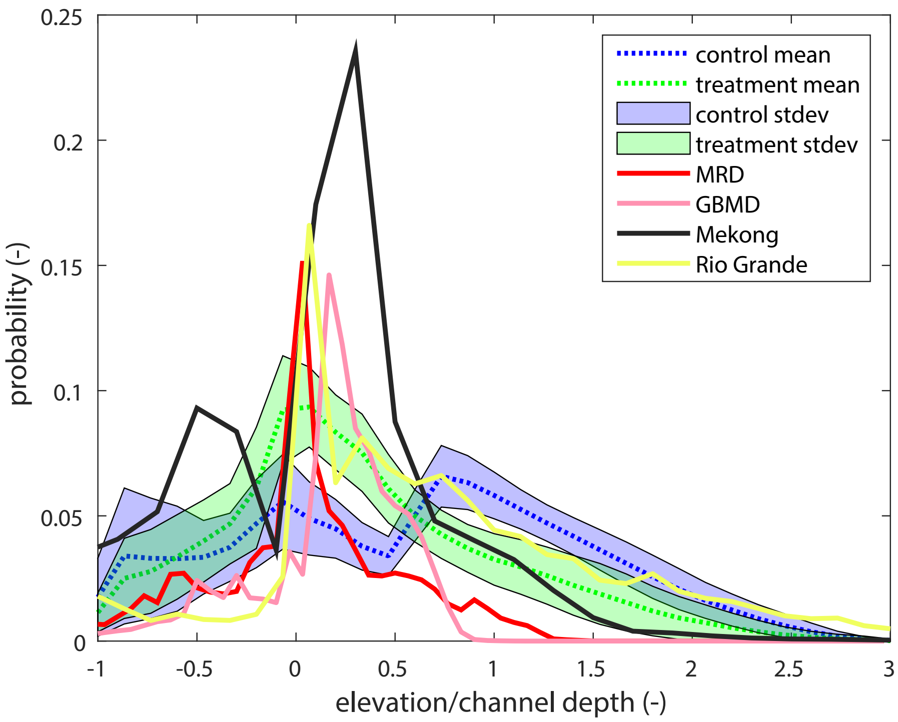

Figure 4: Hypsometry of the control and treatment experiments and four global deltas (Mississippi River [MRD], Ganges Brahmaputra Meghna [GBMD], Mekong, and Rio Grande). Elevation relative to sea level is scaled by the channel depth (x-axis) for comparison between field and experimental scale.

The treatment experiment and global deltas show a peak in elevations between 0 to 0.5 channel depths relative to sea level (rsl), the domain of their marsh platforms. In both the treatment experiment and global deltas, >30% of all elevations between -1 and 3 channel depths lie between 0 and 0.5 channel depths rsl, while the control experiment only has 15% of elevations here. Rather, the control experiment shows its peak around 0.8 channel depths rsl due to increased slopes and associated reduced area near the shoreline. The marsh proxy organizes the treatment experiment's hypsometry to reflect the dominant hypsometric feature of delta systems and is an improvement over the control. At a minimum, this suggests that proxies for non-riverine, elevation-based coastal accumulation can improve the fidelity of laboratory scale models. It also suggests that purely fluvial, lobe based delta deposition is insufficient to understand sedimentation in modern deltas. While organic deposition is a reasonable control on these systems, tidal flat and barrier island reworking should also fundamentally influence delta hypsometry and sediment partitioning in similar ways, because they are also focused deposition near sea level. Succinctly, the coupling of marsh and river delta sediment deposition appears to be essential in shaping global deltas.

4.3 Implications

This work can be used to inform restoration and management plans on river deltas with significant marsh deposition. Successful restoration of deltaic wetlands hinges on understanding delta hypsomtery and the temporal and spatial clastic sediment deposition rates. While marsh sedimentation is relatively continuous in the marsh window, it is important to note that this region accumulates primarily fluvial sediment. The extent of this region is increased due to the feedbacks between the river and marsh. Given the importance of channel-marsh interaction to the mass balance in the treatment experiment and in the absence of other clastic sediment distribution mechanisms (e.g., tides or storms), limiting channel-marsh interaction via leveeing could significantly alter the feedbacks observed here.

Engineered marsh platforms must be consistent with how the wetland platform would grow naturally (Paola et al., 2011). Modern deltas have elevation windows that matter for habitability (higher elevation, fluvial ridges) and others that matter for storm surge protection and biodiversity (lower elevation, marshes). The presence of marsh deposition on the shallow platforms created via river diversions (or other restoration methods) will create mostly land at or near sea level. Thus, the probability distribution of elevations (Figure 2b) will eventually have implications for the extent of storm surges and susceptibility to drowning. Similarly, the change in coastal accumulation rates seen in the treatment experiment has implications for the abiotic, fluvial deposit, particularly for regions above the marsh (i.e., fluvial ridges). Fluvial ridges are typically the most populated region of a river delta, existing solidly above the marsh. Since the interaction between rivers and marshes controls this area partitioning, it should be a significant control on modern deltas and any future river diversions created to support them.

5 Conclusion

We show that the addition of marsh proxy sedimentation in a delta experiment fundamentally alters the mass balance and hypsometry of the resulting delta. Specifically, we find a new control on delta top slope: marsh accumulation. The decreased marsh window slope creates feedbacks that impact the spatial and temporal distribution of riverine sediment, leading to increased area near sea level. The interaction of river and marsh sediment in the treatment experiment leads to a morphological signature more consistent with modern-day river deltas than the control. Since marshes grow to keep pace with relative sea level rise in the low-lying regions of the delta, they fundamentally flatten land near the coast creating the vast marsh platforms seen globally. The lower slopes create feedbacks with clastic sediment deposition patterns that will help to inform future restoration plans, as these plans typically hinge on the successful distribution and retention of riverine sediment.

Acknowledgments

The project was funded in part by an NSF grant (co PIs Kyle Straub; NSF EAR-1848994 that funded Kyle Straub and Jose Silvestre's time plus much of the experimental costs and John Shaw; NSF EAR-1848993 that funded John Shaw and Sam Zapp's time plus some of the experimental costs) and in part by the U.S. Geological Survey (funded Kelly Sanks' hourly work). We have no known conflicts of interest. We would like to thank Dr. Eric Barefoot for his monumental help in automating the treatment experiment.

Open Research

Data and software that reproduce the results of this study are hosted in Zenodo (`https://doi.org/10.5281/zenodo.5911147`) and Github (`https://github.com/kmsanks/TDWB_19_2_MassBalance_Morphology`) repositories.

Data archiving of the raw experimental data is underway and will be available at the "Tulane_Sediment_Dynamics_Stratigraphy_TSDS" project space: `https://sead2.ncsa`

.illinois.edu/spaces/5825f529e4b0f3dd19c8d93a (TDB-18-1 and TDWB-19-2-Surface-Processes) upon review. Note, this data is not needed to reproduce any results from the study, but may be of interest for other researchers. All data used in this study is archived in the Zenodo or Github repositories (see above).

References

Allen, J. (2000, July). Morphodynamics of Holocene salt marshes: a review sketch from the Atlantic and Southern North Sea coasts of Europe. *Quaternary Science Reviews*, *19*(12), 1155–1231. doi: 10.1016/S0277-3791(99)00034-7

Baustian, J. J., Mendelssohn, I. A., & Hester, M. W. (2012). Vegetation's importance in regulating surface elevation in a coastal salt marsh facing elevated rates of sea level rise. *Global Change Biology*, *18*(11), 3377–3382. Retrieved 2021-12-29, from https://onlinelibrary.wiley.com/doi/abs/10.1111/j.1365-2486.2012.02792.x doi: 10.1111/j.1365-2486.2012.02792.x

Bohacs, K., & Suter, J. (1997, October). Sequence Stratigraphic Distribution of Coaly Rocks: Fundamental Controls and Paralic Examples. *AAPG Bulletin*, *81*(10), 1612–1639. Retrieved 2021-06-14, from https://pubs.geoscienceworld.org/aapgbull/article-abstract/81/10/1612/39371/Sequence-Stratigraphic-Distribution-of-Coaly-Rocks doi: 10.1306/3B05C3FC-172A-11D7-8645000102C1865D

Cahoon, D. R., Reed, D. J., & Day, J. W. (1995, October). Estimating shallow subsidence in microtidal salt marshes of the southeastern United States: Kaye and Barghoorn revisited. *Marine Geology*, *128*(1-2), 1–9. Retrieved 2017-04-20, from http://linkinghub.elsevier.com/retrieve/pii/002532279500087F doi: 10.1016/0025-3227(95)00087-F

Caldwell, R. L., & Edmonds, D. A. (2014). The effects of sediment properties on deltaic processes and morphologies: A numerical modeling study. *Journal of Geophysical Research: Earth Surface*, *119*(5), 961–982. Retrieved 2022-01-11, from https://onlinelibrary.wiley.com/doi/abs/10.1002/2013JF002965 doi: 10.1002/2013JF002965

Chesnut, J., & Greb, S. F. (1992, January). Lowstand versus highstand eustatic models for peat preservation: The coal-bearing rocks of the Breathitt Group, Eastern Kentucky. *Geological Society of America, Abstracts with Programs; (United States)*, *24:7*.

Edmonds, D. A., Hoyal, D. C. J. D., Sheets, B. A., & Slingerland, R. L. (2009, August). Predicting delta avulsions: Implications for coastal wetland restoration. *Geology*, *37*(8), 759–762. doi: 10.1130/G25743A.1

Edmonds, D. A., & Slingerland, R. L. (2008). Stability of delta distributary networks and their bifurcations. *Water Resources Research*, *44*(9). Retrieved 2021-06-14, from https://agupubs.onlinelibrary.wiley.com/doi/abs/10.1029/2008WR006992 doi: 10.1029/2008WR006992

Edmonds, D. A., & Slingerland, R. L. (2010, February). Significant effect of sediment cohesion on delta morphology. *Nature Geoscience*, *3*(2), 105–109. doi: 10.1038/ngeo730

Ericson, J., Vorosmarty, C., Dingman, S., Ward, L., & Meybeck, M. (2006, February). Effective sea-level rise and deltas: Causes of change and human dimension implications. *Global and Planetary Change*, *50*(1-2), 63–82. Retrieved 2017-04-20, from http://linkinghub.elsevier.com/retrieve/pii/S0921818105001827 doi: 10.1016/j.gloplacha.2005.07.004

Esposito, C. R., Shen, Z., Törnqvist, T. E., Marshak, J., & White, C. (2017, July). Efficient retention of mud drives land building on the Mississippi Delta plain. *Earth Surface Dynamics*, *5*(3), 387–397. Retrieved 2021-06-14, from https://esurf.copernicus.org/articles/5/387/2017/ doi: 10.5194/esurf-5-387-2017

Holmquist, J. R., Windham-Myers, L., Bliss, N., Crooks, S., Morris, J. T., Megonigal, J. P., … Woodrey, M. (2018, June). Accuracy and Precision of Tidal Wetland Soil Carbon Mapping in the Conterminous United States. *Scientific Reports*, *8*(1), 9478. Retrieved 2022-01-21, from `https://www.nature.com/articles/s41598-018-26948-7` (Bandiera_abtest: a Cc_license_type: cc_by Cg_type: Nature Research Journals Number: 1 Primary_atype: Research Publisher: Nature Publishing Group Subject_term: Carbon cycle;Climate-change mitigation Subject_term_id: carbon-cycle;climate-change-mitigation) doi: 10.1038/s41598-018-26948-7

Hoyal, D. C. J. D., & Sheets, B. A. (2009). Morphodynamic evolution of experimental cohesive deltas. *Journal of Geophysical Research: Earth Surface*, *114*(F2). doi: 10.1029/2007JF000882

Kirwan, M. L., Guntenspergen, G. R., D'Alpaos, A., Morris, J. T., Mudd, S. M., & Temmerman, S. (2010, December). Limits on the adaptability of coastal marshes to rising sea level: ecogeomorphic limits to wetland survival. *Geophysical Research Letters*, *37*(23). Retrieved 2017-04-20, from `http://doi.wiley.com/10.1029/2010GL045489` doi: 10.1029/2010GL045489

Kirwan, M. L., & Murray, A. B. (2007, April). A coupled geomorphic and ecological model of tidal marsh evolution. *Proceedings of the National Academy of Sciences*, *104*(15), 6118–6122. Retrieved 2017-04-20, from `http://www.pnas.org/cgi/doi/10.1073/pnas.0700958104` doi: 10.1073/pnas.0700958104

Li, Q., Benson, W. M., Harlan, M., Robichaux, P., Sha, X., Xu, K., & Straub, K. M. (2017). Influence of Sediment Cohesion on Deltaic Morphodynamics and Stratigraphy Over Basin-Filling Time Scales. *Journal of Geophysical Research: Earth Surface*, *122*(10), 1808–1826. doi: 10.1002/2017JF004216

Li, S., Wang, G., Deng, W., Hu, Y., & Hu, W. (2009, December). Influence of hydrology process on wetland landscape pattern: A case study in the Yellow River Delta. *Ecological Engineering*, *35*(12), 1719–1726. Retrieved 2021-08-22, from `https://www.sciencedirect.com/science/article/pii/S0925857409002122` doi: 10.1016/j.ecoleng.2009.07.009

Minderhoud, P. S. J., Coumou, L., Erkens, G., Middelkoop, H., & Stouthamer, E. (2019, August). Mekong delta much lower than previously assumed in sea-level rise impact assessments. *Nature Communications*, *10*(1), 3847. Retrieved 2021-06-08, from `https://www.nature.com/articles/s41467-019-11602-1` doi: 10.1038/s41467-019-11602-1

Morris, J. T., Sundareshwar, P. V., Nietch, C. T., Kjerfve, B., & Cahoon, D. R. (2002, October). Responses of Coastal Wetlands to Rising Sea Level. *Ecology*, *83*(10), 2869–2877. doi: 10.1890/0012-9658

Nyman, J. A., Walters, R. J., Delaune, R. D., & Patrick, W. H. (2006, September). Marsh vertical accretion via vegetative growth. *Estuarine, Coastal and Shelf Science*, *69*(3), 370–380. Retrieved 2021-06-14, from `https://www.sciencedirect.com/science/article/pii/S0272771406001843` doi: 10.1016/j.ecss.2006.05.041

Paola, C., Straub, K., Mohrig, D., & Reinhardt, L. (2009, December). The "unreasonable effectiveness" of stratigraphic and geomorphic experiments. *Earth-Science Reviews*, *97*(1), 1–43. Retrieved 2020-08-12, from `http://www.sciencedirect.com/science/article/pii/S001282520900083X` doi: 10.1016/j.earscirev.2009.05.003

Paola, C., Twilley, R. R., Edmonds, D. A., Kim, W., Mohrig, D., Parker, G., … Voller, V. R. (2011). Natural processes in delta restoration: application to the Mississippi Delta. *Annual Review of Marine Science*, *3*, 67–91. doi: 10.1146/annurev-marine-120709-142856

Parker, G., Paola, C., Whipple, K. X., & Mohrig, D. (1998, October). Alluvial Fans Formed by Channelized Fluvial and Sheet Flow. I: Theory. *Journal of Hydraulic Engineering*, *124*(10), 985–995. Retrieved 2021-10-12, from `https://`

ascelibrary.org/doi/abs/10.1061/(ASCE)0733-9429(1998)124:10(985) doi: 10.1061/(ASCE)0733-9429(1998)124:10(985)

Powell, E. J., Kim, W., & Muto, T. (2012). Varying discharge controls on timescales of autogenic storage and release processes in fluvio-deltaic environments: Tank experiments. *Journal of Geophysical Research: Earth Surface*, *117*(F2). Retrieved 2022-01-12, from https://onlinelibrary.wiley.com/doi/abs/10.1029/2011JF002097 doi: 10.1029/2011JF002097

Ratliff, K. M., Hutton, E. W. H., & Murray, A. B. (2021, April). Modeling long-term delta dynamics reveals persistent geometric river avulsion locations. *Earth and Planetary Science Letters*, *559*, 116786. Retrieved 2021-09-17, from https://www.sciencedirect.com/science/article/pii/S0012821X21000455 doi: 10.1016/j.epsl.2021.116786

Sanks, K. M., Shaw, J. B., & Naithani, K. (2020). Field-Based Estimate of the Sediment Deficit in Coastal Louisiana. *Journal of Geophysical Research: Earth Surface*, *125*(8). doi: 10.1029/2019JF005389

Smart, J. S., & Moruzzi, V. L. (1971, January). *Quantitative Properties of Delta Channel Networks* (Tech. Rep.). IBM Thomas J Watson Research Center, Yorktown Heights, NY.

Straub, K. M., Paola, C., Mohrig, D., Wolinsky, M. A., & George, T. (2009, September). Compensational Stacking of Channelized Sedimentary Deposits. *Journal of Sedimentary Research*, *79*(9), 673–688. Retrieved 2022-01-11, from https://doi.org/10.2110/jsr.2009.070 doi: 10.2110/jsr.2009.070

Whipple, K., Parker, G., Paola, C., & Mohrig, D. (1998, November). Channel Dynamics, Sediment Transport, and the Slope of Alluvial Fans: Experimental Study. *The Journal of Geology*, *106*(6), 677–694. Retrieved 2022-01-17, from https://www.journals.uchicago.edu/doi/10.1086/516053 doi: 10.1086/516053

Wickert, A. D., Martin, J. M., Tal, M., Kim, W., Sheets, B., & Paola, C. (2013). River channel lateral mobility: metrics, time scales, and controls. *Journal of Geophysical Research: Earth Surface*, *118*(2), 396–412. Retrieved 2022-01-11, from https://onlinelibrary.wiley.com/doi/abs/10.1029/2012JF002386 doi: 10.1029/2012JF002386

1 Experimental Design

1.1 Boundary Conditions

The control and treatment experiments were conducted in the Tulane Sediment Dynamics laboratory. The control experiment was conducted in the delta basin in 2018 and the treatment experiment was conducted in the deep water basin in 2019. Both the control and treatment experiments had the exact same boundary conditions, except the treatment experiment had marsh deposition and the control experiment did not (Table 1). Thus, any changes between the two experiments can be attributed directly to the addition of the marsh.

Table 1: Experiment boundary conditions. The experimental conditions for both the control (no marsh) and treatment (marsh deposition) experiments used for comparison in this study.

Boundary Condition	**Control**	**Treatment**
Sediment Mixture	Hoyal and Sheets (2009)	Hoyal and Sheets (2009)
Realtive Sea Level Rise ($RSLR_b$)	0.25 mm/hr	0.25 mm/hr
Riverine Sediment Discharge (Q_s)	1.41 kg/hr	1.41 kg/hr
Riverine Water Discharge (Q_w)	$1.72*10^{-4}$ m^3/s	$1.72*10^{-4}$ m^3/s
In-situ Marsh Deposition (Q_m)	None	150 g/hr (total) 3.7 g/hex (max production) 1.7 g/hex (stable/unstable)

1.2 Data and Marsh Proxy

We expand here on details of the data collection and marsh distribution. Because the treatment experiment was not fully automated, we paused the experiment for ∼10 hours each night. During the progradation phase, overnight subsidence was tested by taking a LiDAR scan at the end of the day and beginning of the next day to observe changes in elevation. No detectable subsidence was observed when the experiments were paused overnight, thus pausing of the experiment did not impact the elevation data collected in comparison to the control.

We deposited the marsh sediment with about 50% accuracy. An average of 200 g of kaolinite was deposited per deposition hour, which is less than the average ideal deposition rate (calculated via the model) of 260 g per deposition (main text Figure 1d). The reasons for this were (1) compaction of the kaolinite in the sieve and (2) dampening of the ButtKicker^{TM} signal that caused apparent uneven deposition through time. We mitigated this by switching the direction of the deposition every two hours (e.g., the first hour the sieve moved from left to right across the basin to deposit marsh and the second hour the sieve moved from right to left). We also re-calibrated the sediment dispenser after each depositional cycle. Though less accurate than anticipated, the deposition of marsh proxy altered the morphology and surface processes of the delta.

2 Deltaic sediment balance

We calculate the sediment volume balance for both the control and treatment experiments in order to directly compare the volume and rate of sediment storage throughout the delta. While this comparison is revealing, we are specifically interested in the influence of marsh sedimentation on delta volume balance; thus, we need to quantify the volume of the riverine and marsh sediment (kaolinite clay) in the treatment experiment throughout its entirety. Due to compaction of the marsh sediment, erosion, and deposition of both marsh and river sediment in the same area on the delta top, we cannot directly quantify the sediment accumulation using the LiDAR scans. Instead, we take advantage of the preserved stratigraphy to determine the marsh volume.

2.1 Stratigraphic Interpolation

The resulting stratigraphy was split into two sections to acquire one cross-section along dip. Then the deposit was sectioned from distal to proximal along strike every 10 cm. Photographs were taken of each section and color image processing was used to obtain a marsh fraction and thickness roughly every 10 cm (Figure 1a).

Using this gridded stratigraphic data, we use Bayesian kriging techniques ("Bayesian inference", 2007) to interpolate a pixel (5 mm x 5 mm) marsh fraction and marsh thickness for the entire delta basin (Figure 1b and c). Bayesian kriging is a useful interpolation technique because it integrates data and model to predict values and uncertainty on those predicted values ("Bayesian inference", 2007). Further, it is less likely to be biased than traditional interpolation techniques, producing a more accurate model ("Bayesian inference", 2007).

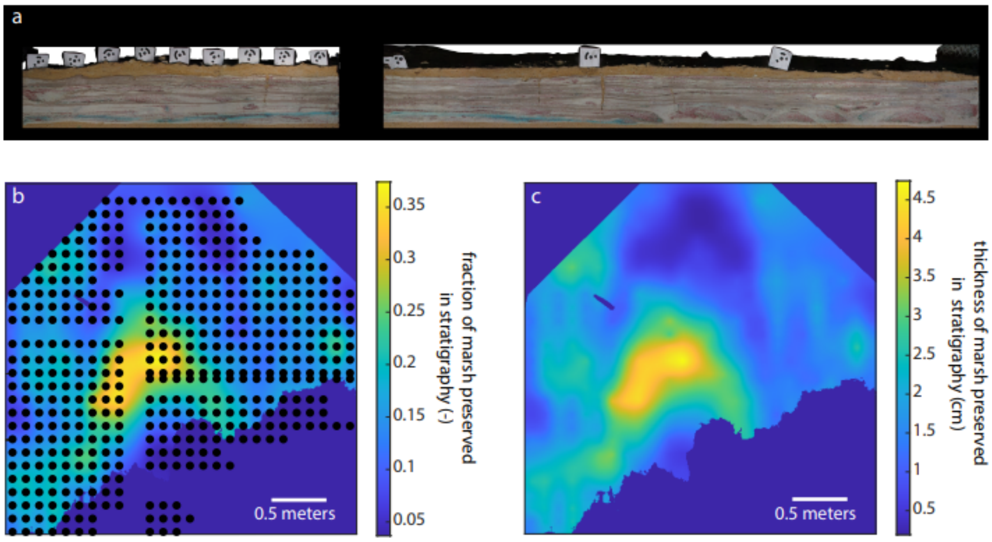

Figure 1: Stratigraphic Interpolation. (a) An along strike section of the treatment experiment at 1.1 m from the entrance channel. The targets on the left one-third of the image are spaced 10 cm apart and thickness and fraction of marsh was collected for the entire deposit below each target. The red sediment is channel sand, white is channel floodplain, and brown is marsh. The tan sediment above and below the section is play sand and not part of the delta deposit. (b) The interpolated fraction of marsh sediment that is preserved in stratigraphy for the area above -9 mm relative to seal level for at least 10% of the experiment. The black dots represent the measured values of marsh fraction and thickness and are roughly 10 cm apart. The raw data (black dots) was interpolated using a 5 mm x 5 mm grid (the resolution of the LiDAR data). (c) The intepolated thickness of marsh sediment that is preserved in the stratigraphy (cm) using a 5 mm x 5 mm grid.

2.2 Volume Balance

The volume balance for the different zones (e.g., above marsh, marsh window, delta top) was calculated using the final resulting stratigraphy. We define the region above the marsh as the area that is above 5 mm relative to sea level (rsl) for at least 90% of the experiment to minimize the influence of marsh on sedimentation of this region in the treatment experiment. The marsh window is the area $\leq$5 mm rsl and $\geq$-9 mm rsl for greater than 10% of the experiment. By using this criteria, the marsh window begins exactly where the above marsh zone ends. Finally, we define the delta top as the area that is $\geq$ -9 mm rsl for at least 50% of the experiment. This region then encompasses a smaller extent than the combined above marsh and marsh window area. However, we use this region to compare the average delta top area and volume of the two experiments.

We calculate the volume balance for all three zones using the following logic. Total sediment accumulated ($\mathrm{V_T}$; $\mathrm{mm^3}$) at each pixel (i) is given by:

$$V_T = (Z_{final} - Z_{initial}) * A_{pixel}, \tag{1}$$

where $\mathrm{z_{final}}$ is the pixel elevation of the last LiDAR scan, $\mathrm{z_{initial}}$ is the pixel elevation of the first LiDAR scan, and $\mathrm{A_{pixel}}$ is the area of one pixel (25 $\mathrm{mm^2}$). From there, we multiply by the interpolated marsh fraction ($\mathrm{f_m}$; -) to determine the marsh sediment accumulated ($\mathrm{V_m}$; $\mathrm{mm^3}$), given by:

$$V_m = f_m * V_T. \tag{2}$$

The clastic (riverine) sediment accumulated (V_c; mm^3) is then:

$$V_c = V_T - V_m. \tag{3}$$

Note that because the control experiment has no marsh deposition, V_m is 0 and V_c is simply equal to V_T. Refer to Table 1 in the main text for the zonal volume balance.

We compared the zonal mass balance for the area above the marsh to a mass balance calculated using a moving average above the marsh window. The moving window shows a sediment accumulation rate of 0.202 m^3 and 0.0655 m^3 for the control and treatment experiments, respectively. While this is about a 40% difference from the integrated zonal volume, both methods show a similar percent difference in volume between the two experiments. We integrated through time for each of the three zones (above marsh, marsh, and delta top) because even though the delta is in equilibrium, autogenic variability impacts short-term sediment depositon and resulting stratigraphy (i.e., the moving average does not account for long- or short-term compactional subsidence) (Jerolmack & Sadler, 2007).

The trapping efficiency (TE; %) is defined by:

$$TE = \frac{V_c}{V_D} * 100, \tag{4}$$

where V_D (a constant 0.660 m^3) is the clastic sediment delivered to the delta top and calculated by:

$$V_D = (\frac{flux}{\rho} * t) * 10^{-6}, \tag{5}$$

where flux is the sediment being delivered to the system by the river (a constant 1406.14 g/hr), t is the entire run time of the experiment (560 hrs), and ρ is the bulk density of the clastic sediment (a constant 1.19 g/cm^3), assuming an average 55% porosity (mean of cores taken from the control experiment) and a particle density of 2.65 g/cm^3.

In Table 1 of the main text, we calculate two TE for the marsh window. The TE descried by footnote a in Table 1 is the TE calculated using the clastic sediment delivered to the marsh window (V_{Dm}) instead of the clastic sediment delivered to the delta top (V_D):

$$V_{Dm} = V_D - V_{am}, \tag{6}$$

where V_{am} is the total clastic sediment accumulated above the marsh window.

3 Delta Hypsometry

We compare the hypsometry (elevation distribution) of the control and treatment experiments to the hypsometry of three vegetated and one non-vegetated field-scale deltas. In order to compare the experimental scale to the field scale, we non-dimensionalize the elevations of the delta top by dividing elevation by one average channel depth for the given system. The channel depths used are 15 mm for the experiments, 30 m for the Missississippi River Delta (MRD) and the Ganges Brahamaputra Meghna Delta (GBMD), 10 m for the Mekong River Delta, and 15 m for the Rio Grande River Delta. Notably, we see a more similar hypsometric signature between the treatment and global deltas, as compared to the control. The treatment and gloabl deltas have >30% of their elevations between 0 and 0.5 channel depths above sea level. Specifically, the treatment experiment has 31%, MRD has 44%, GBMD has 64%, Mekong River Delta has 50%, and Rio Grande River Delta has 38% of elevations here. Comparatively, the control only has 17% of elevations in this 0 to 0.5 channel depths above sea level window. Rather, the control has a bi-modal distribution with peaks at 0.06 channel depths below sea level and 0.733 channel depths above sea level.

The elevation data for the field scale deltas was collected using ETOPO Global Relief Model (NOAA) in Google Earth Engine (GEE). GEE provides an interactive software, which we used to create polygons of the delta tops of three vegetated deltas (the Mississippi River Delta, Ganges Brahamaputra Meghna Delta, and Mekong River Delta), and one mostly unvegetated delta (the Rio Grande River Delta) (Figure 2).

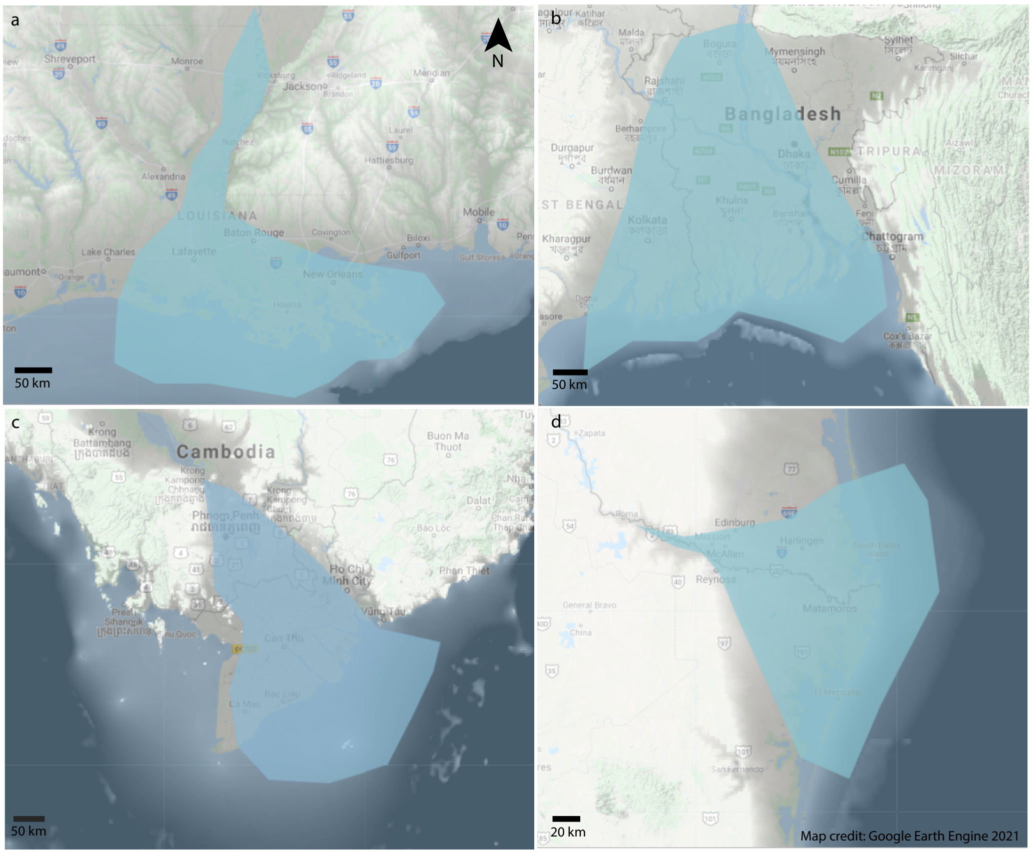

Figure 2: Delta polygons. The satellite and topographic data for the field-scale deltas used in the hypsometric analysis and the corresponding polygons (blue) used to obtain elevation data. (a) The Mississippi River Delta located in Louisiana, USA. (b) The Ganges Brahamaputra Meghna Delta located in Bangladesh and West Bengal, India. (c) The Mekong River Delta located in Cambodia and Vietnam. (d) The Rio Grande River Delta located on the border of southeast Texas, USA and northeast Mexico. The scales vary on each map, but the north arrow and credits are the same for all.

The polygons were created with the following rules. (1) We avoided locations that were greater than 3 channel depths above to sea level and less than 1 channel depth below sea level, (2) we attempted to determine the entrance of the channel into the "delta top", and (3) we made sure to include the main distributary channels within the polygon area. While the areas were chosen somewhat arbitrarily, we tested different polygons for the same delta and did not observe a significant difference in the histogram distribution shape, thus we are confident in the patterns observed in Figure 4 (main text).

References

Bayesian inference. (2007). In P. J. Diggle & P. J. Ribeiro (Eds.), *Model-based Geostatistics* (pp. 157–198). New York, NY: Springer. Retrieved 2021-08-22, from `https://doi.org/10.1007/978-0-387-48536-2_7` doi: 10.1007/978-0-387-48536-2_7

Jerolmack, D. J., & Sadler, P. (2007). Transience and persistence in the depositional record of continental margins. *Journal of Geophysical Research: Earth Surface*, *112*(F3). Retrieved 2021-10-12, from `https://onlinelibrary.wiley.com/doi/abs/10.1029/2006JF000555` doi: 10.1029/2006JF000555